

# Effect of Molecular Weight, Branching, and Free Volume on Diffusion in Epoxies during Curing<sup>†</sup>

Weiching Yu and Ernst D. von Meerwall\*

Department of Physics and Institute of Polymer Science, University of Akron,  
Akron, Ohio 44325. Received April 17, 1989; Revised Manuscript Received July 24, 1989

**ABSTRACT:** We have used the pulsed-gradient spin-echo method to measure diffusivity  $D$  in two epoxy systems, DGEBA and DGEBA (Shell Epon 828), as function of time during curing with DDS at 120 and 140 °C. Diffusion of the polymer as well as curative and probe molecules (5% unreactive impurities in DGEBA; 8% plasticizer DBP in Epon 828) was observed from the melt to beyond gelation. Parallel IR determinations of the conversion  $x$  of the curing reaction and use of branching theory allowed approximate modeling of the molecular weight ( $M$ ) distribution of the emerging aggregates, whose corresponding  $D$  distribution was found to be in agreement with the data. While the average  $D$ (polymer) decreases by some 3 orders of magnitude during the cure, the decrease of  $D$ (probe), arising from changes in chain-end free volume alone, is smaller. After correction for these free-volume changes  $D$ (polymer) is found to depend much more strongly on  $M$  of the growing aggregates than the prediction of the Rouse model. These results suggest that branching of the diffusing molecules and their equivalent host environment has considerable influence on the friction coefficient in these unentangled systems at least up to gelation. In both systems  $D$  data at the two temperatures follow a common curve  $D(x)/D(0)$  vs  $x$ , consistent with the hypothesis that the progress of curing after its initial stages is largely controlled by diffusion. Differences in diffusion behavior between systems are attributed to differences in  $M$  and chain flexibility.

## I. Introduction

The importance of epoxies derives from their use in several separate but related contexts, e.g., as adhesives, as protective layers in the form of paints and coatings, and as matrix materials for composites used in structural applications. In most of these the epoxy ultimately forms a glassy network that may incorporate, or adhere to, discrete foreign objects or dispersed phases of another polymer. The process of curing to produce the network has a profound influence on the properties of the finished materials and has long been the subject of detailed study.

During isothermal curing epoxies traverse a sol-gel and a vitrification transition; this process is generally described in terms of a time-temperature transition (T-T-T) diagram.<sup>1</sup> As the cure progresses, monomers combine to form dimers, trimers, etc., which then proceed to link into branched aggregates, and finally form a cross-linked gel, into which most of the remaining sol may be incorporated. The glass transition temperature  $T_g$ , descriptive of the loss of free volume and thus of overall molecular mobility, increases with cure but at a rate that depends on the stage of curing. The cure kinetics, at first rapid and controlled mainly by the rate of the chemical reaction, slows down and in the later stages of curing becomes limited by the rapidly decreasing diffusion rate of the remaining larger unreacted entities in the presence of the more constraining branched and/or entangled sol and cross-linked network.

Several types of experiment have been used to study curing in epoxies or similar systems. Rheological measurements such as storage modulus and viscosity<sup>2</sup> are particularly effective in describing changes in long-range cooperative motions, e.g., near the gel transition. For the study of somewhat shorter range interactions between the growing molecules, microviscosity as determined by fluorescence, e.g., of a viscosity-sensitive probe,<sup>3</sup> polarization,<sup>4</sup> chemiluminescence,<sup>5</sup> and excimer emission<sup>6</sup> are well suited.

Direct measurements of molecular self-diffusion (Brownian motion) are beginning to be applied to the study of curing; fluorescence recovery after photobleaching (FRAP) has been used<sup>3</sup> to study the diffusion of chemically labeled free probe molecules dissolved in a curing matrix. Subtle changes in dielectric properties during curing can result from the attendant loss of mobility of ionic impurities.<sup>7</sup>

The photoisomerization of azochromophores at different sites<sup>8</sup> along a molecule was employed to probe the motion of a submolecule, and the results were interpretable in terms of the distribution of free volume within a curing system. ESR and positronium annihilation spectroscopies have also been applied to describe the mobility and free volume of a cured polymer matrix.

Of particular promise in the study of curing is nuclear magnetic resonance (NMR), not merely in its spectroscopic variety as an aid in determining the time-dependent concentration of a moiety involved in the curing reaction,<sup>9</sup> but increasingly as a tool to study molecular mobility directly. The spin-spin relaxation time  $T_2$  has recently been used as a sensitive probe of molecular mobility of both sol and gel in rubbery networks and composites as function of departure from curing stoichiometry and of filler particle size.<sup>10</sup> Spin-spin and spin-lattice relaxation rates have been measured to characterize molecular motions in epoxy (DGEBA) as melts,<sup>11</sup> and networks,<sup>12</sup> as well as during curing.<sup>13</sup> The NMR-based pulsed-gradient spin-echo (PGSE) method rapidly measures long-range self-diffusion of entire molecules. It is possible simultaneously to measure the diffusion of naturally occurring polymer sol and curing agent plus unreactive monomer without the need for chemical labeling; a curing study of a rubbery polybutadiene<sup>14</sup> and a combined study of  $T_2$  and diffusion in cured PB networks<sup>10</sup> using this method have been described. Earlier post-cure PGSE work in composites<sup>15</sup> concentrated on the restriction and reduction of the diffusivity of small probe molecules in response to various attributes of the filler particles.

The present work reports a PGSE diffusion study of two epoxies differing in molecular weight, DGEBA and DGEBA, during curing with DDS, at both 120 and 140

<sup>†</sup> Supported in part by the National Science Foundation (Grant DMR-8706166) and by Thiokol Corp.

Table I  
Characteristics of Molecular Species

species	$M$ , dalton	$\bar{M}_w/\bar{M}_n$ via GPC <sup>a</sup>	$f^b$	descriptn
DGEB monomer	202		$E = 2$	reactive monomer constituting 95 wt % of DGEB as supplied
DGEB impurity	(~200)		$E = 0$	unreactive monomers (>90% 1,4-butanediol) 5 wt % present in DGEB
DGEBA	$\bar{M}_n = 411$	1.09 <sup>c</sup>	$E = 2$ (nom)	>99% molecule with $E > 0$
DBP	278		0	plasticizer; aromatic, 8 wt % used with DGEBA
DDS	248		$A = 4$ (nom)	curing agent, 99.8% pure, constituting 37 wt % in DGEB system <sup>d</sup> and 21 wt % in DGEBA system

<sup>a</sup> Via Waters HPLC at 25 °C in THF; ultrastaygel columns. <sup>b</sup> Functionality (average) in terms of amines ( $A$ ) or epoxides ( $E$ ) per molecule. <sup>c</sup> Shell Epon 828 nominally contains 75%  $M = 340$  and 25%  $M = 624$ . <sup>d</sup> Initial fractional DDS content in the batches to be cured, assuming  $A/E = 1$  (molecular ratio epoxy:DDS = 2:1) and including weight of nonreactive species.

°C, from cure initiation to beyond the gel point. These temperatures were chosen, after several trials, to be high enough to permit diffusion measurements well into the intermediate stages of curing, i.e., until the rising glass transition prevented further measurements, but as low as possible to minimize exothermal sample heating during curing and to provide sufficient time for precise diffusion measurements. A parallel determination of the extent of the curing reaction based on infrared absorption spectroscopy makes possible an approximate description of the statistical properties of the reacting aggregates. Diffusion of probe molecules is included in our measurements and serves to describe the change in free volume during curing.

On the basis of contemporary theories of polymer rheology, an attempt is made to partition the polymer diffusion rate into contributions from free volume, their own increasing molecular weight, the increasing resistance of the emerging network to molecular transport, and the direct topological effect of branching. The last two of these effects are not well understood, so that it will not be possible to assign their appropriate fractional contributions to diffusant vs host effects. However, it will become clear that the conventional Rouse model, whose predictions for self-diffusion apply to branched as well as unbranched solutions of polymers in this molecular weight range, is not capable of explaining these observations in our concentrated systems. Preliminary reports of this work have been given.<sup>16,17</sup>

## II. Experiment and Data Analysis

**A. Samples.** Diglycidyl ether of Bisphenol A (DGEBA) prepared by Shell Chemical Co. as Epon 828 was used as received and was mixed with 8% of a plasticizer, dibutylphthalate (DBP), to obtain a blend containing a molecularly similar probe species. As a comparable system of smaller molecular weight, diglycidyl ether 1,4-butanediol (DGEB) was used as purchased from Aldrich Chemicals, Inc.; this product is known to contain 5% of unreactive species, which served as plasticizer as well as probe in the NMR investigation. Gel permeation chromatography was used to confirm the impurity content and obtain the molecular weight distribution of the reactive bulk epoxides, information helpful in the reduction of the PGSE data. Samples were eluted at a flow rate of 1.0 mL/min in tetrahydrofuran at 25 °C using a Waters HPLC component system equipped with ultrastaygel columns (Waters: 500, 10<sup>3</sup>, 10<sup>4</sup>, and 10<sup>5</sup> Å). For Epon 828 two sharp peaks were observed and identified in terms of the two known subspecies, of molecular weights 340 ( $n = 0$ ) and 624 Da ( $n = 1$ ); the relative amounts were consistent with the manufacturer's nominal ratio of 3:1. In DGEB a single slightly broadened peak was observed. The molecular characteristics of these species are summarized in Table I.

The preheated epoxies containing probe molecules were stoichiometrically mixed at 100 °C with 4,4'-diaminodiphenyl sulfone (DDS) obtained from Aldrich Chemicals, for approximately 4 min, at which time the mixtures had become transparent. The preparations were immediately cooled and divided

for use in the IR and PGSE studies. PGSE specimens required some 300 mg of material to be placed at the bottom of 7-mm o.d. NMR sample tubes, which were flushed with N<sub>2</sub> gas and sealed. These samples were kept at -15 °C until required several days later, when they were placed in the preheated NMR probe, this moment being regarded as the beginning of the cure (see below). The first PGSE measurement was begun within less than 5 min; several hours later continued measurements became impossible when the specimen's rising glass transition temperature approached and exceeded the temperature of the experiment. As expected on the basis of the known chemical compatibility of the ingredients, no evidence of phase separation was detected in either system at any stage of curing.

**B. IR Curing Study.** The extent of the curing reaction was monitored as a function of time via parallel infrared absorption measurements on aliquots taken from the same batches used in the PGSE work. One drop of fresh sample was squeezed between circular NaCl plates separated by a 15-μm PTFE spacer. The disappearance of the characteristic epoxide absorption peak at 915 cm<sup>-1</sup> was monitored on a Beckman FT 2100 FTIR instrument. Temperatures identical with those used in the diffusion experiments (120.2 and 140.2 °C) were maintained to a precision of ±0.2 °C. To correct for sample thickness fluctuations during cure two internal reference peaks were chosen for each system. One common to both systems, arising from the phenyl ring stretch in DDS, was centered at 1610 cm<sup>-1</sup> and the other either at 1184 cm<sup>-1</sup> due to C—C stretching of the bridge carbons in DGEBA or at 1723 cm<sup>-1</sup> due to the C=O stretch in DBP dissolved in the DGEB system. The extent  $x_e$  of the curing reaction, in terms of epoxy groups, was then calculated from the areas  $A$  of the absorption peaks after suitable subtraction of a manually interpolated curved base line arising from neighboring peaks:

$$x_e(t) = 1 - \frac{A_{915}(t) A_{ref}(0)}{A_{915}(0) A_{ref}(t)} \quad (1)$$

The reference peak area ratios in each system were obtained for both peaks, checked for consistency, and averaged for use in eq 1. No significant differences in  $x_e(t)$  were observed when the experiments were repeated with samples taken from left-over NMR portions of these batches, kept as extremely viscous liquids at -15 °C for between 1 and 2 weeks, showing that the NMR samples had not yet significantly reacted at the beginning of their curing study. The experimental uncertainty in  $x_e$  from all sources was estimated to be ±6% of  $x_e$  for  $x_e \geq 0.4$ , approaching a constant ±0.03 at lower  $x_e$ .

To obtain some of the moments of a theoretical molecular weight distribution at any  $x_e$  prior to gelation for the functionalities involved, appropriate branching theory was used.  $\bar{M}_w(x)$  was evaluated as function of  $x$  from an expression derived by Dušek and Ilavský<sup>18</sup> under the reasonable assumption that no side reactions occur. The temperature in use in our experiments seem too low for reactions such as etherification of epoxide and hydroxyl groups to become significant prior to gelation. Estimates of  $\bar{M}_w(x)$  were obtained by evaluating the theory of Miller and Macosko,<sup>19</sup> with two additional assumptions, i.e., that no intramolecular reactions (e.g. cyclization) occur in the finite species and that the primary and secondary amine groups are equally reactive. While the first of these assumptions is

likely to be satisfied here, the second is not;<sup>20,21</sup> the main effect of its invalidity is an upward shift of the stoichiometric gel point from  $x_{\text{gel}} = 0.57$  to  $x_{\text{gel}} = 0.58$  in the ideal case but more likely nearer to 0.6 since the amines may be subject to substitution effects.

The molecular weight averages were required for the modeling and interpretation of the diffusivity distributions observed in the PGSE experiments, as will be described below. However, no part of our data reduction or analysis makes use of a quantitative value of  $x_{\text{gel}}$ ; the onset of gelation near  $x = 0.6$  was not evident in the diffusion results (see below) but was clearly inferred from the abrupt change in mechanical properties informally observed in several specimens used for preliminary trials.

**C. Diffusion Study.** Diffusion measurements were made in the proton NMR at 33 MHz using the principal spin echo. The pulsed-gradient spin-echo (PGSE) method<sup>22</sup> extracts self-diffusion (Brownian motion) coefficients from the decrease in the amplitude of the NMR echo in response to a pair of matched, calibrated magnetic field gradient pulses coordinated with the rf pulse sequence. The PGSE method, including the contemporary large-gradient variety in use here, is exhaustively reviewed in the literature;<sup>23</sup> our instrumentation,<sup>24</sup> experimental practices,<sup>25</sup> and data reduction models and software<sup>14,26</sup> were used as described in previous publications, with various refinements. The experiments were conducted at a fixed echo time  $\tau = 25$  ms equal to the gradient pulse spacing  $\Delta$ , and a fixed gradient pulse magnitude  $G = 125$  or  $310$  G/cm; the latter was used at the lower temperature. The gradient pulse duration  $\delta$  was varied between 0 and 16 ms in eight to fifteen steps. A steady gradient  $G_0 = 0.80$  G/cm, parallel to  $G$ , was applied at all times to sharpen and stabilize the echo.

The NMR probe containing the samples under investigation during curing was maintained at the desired curing temperature of 120.2 or 140.2 °C within an accuracy of  $\pm 0.2$  °C and a stability of  $\pm 0.1$  °C over the duration of the experiment. The probe temperature was monitored 3-mm downstream of the sample with the airflow temperature actively regulated so that primary effects of adiabatic sample heating were eliminated. Any temperature difference between the outside and center of the samples was easily estimated to be smaller than the accuracy of the temperature control: the diameter of the cylindrical sample wetting the glass sample tube was only 5 mm, and the rate of heat generation was relatively low since at these low temperatures between 2 and 8 h elapsed between the beginning of curing and estimated gelation.

Diffusional echo attenuations were recorded as rapidly as possible, using minimal signal averaging (three to six echoes per pulse duration setting). One set of echo attenuations was collected within 3 min or less; small signal amplitude drift during each set was later corrected for the changing spin-spin relaxation time  $T_2$ , which was measured between the diffusion experiments. The cycle was repeated every 7–14 min until the spin echo at  $2\tau = 50$  ms decreased in signal-to-noise ratio to less than approximately 3; one such curing run took 6–10 h at 120 °C or 2–4 h at 140 °C.

It has been shown<sup>22</sup> that the slope of a plot of the logarithm of the echo amplitude versus a combined gradient parameter  $(\delta G)^2 (\Delta - \delta/3)$ , with minor corrections involving  $G_0$ , equals  $-\gamma^2 D$ , where  $\gamma$  is the gyromagnetic ratio of the nuclei at resonance, provided their molecules diffuse at the single self-diffusion rate  $D$ . Our echo attenuation data did not adhere to this restriction and thus required analysis by our off-line data reduction and model fitting code<sup>14,26</sup> DIFFUS5, operating on an IBM 9000 workstation. Its most recent modification is a calibrated correction for the effects of short-term residual magnetic field gradients,<sup>27</sup> which can become important at short diffusion times and low diffusion coefficients. In the present investigation, this correction resulted in downward changes in the measured diffusion coefficients of no more than 3%, less than the uncertainties in  $D$ . These amounted to some 4% from imprecision in the gradient calibration, with additional contributions due to correlations in the fits of multicomponent diffusion models (see below) and adverse signal-to-noise conditions; no single  $D$  value to be presented is believed to be uncertain by more than  $\pm 15\%$ .

Near the beginning of curing, few polymer molecules have

reacted; the polydispersity still resembles its initial profile and the free curative (initially present in comparatively large concentrations; see Table I), the probe molecules (unreactive monomer or plasticizer), and the smaller polymer molecules all diffuse at similar but not identical rates. The data reduction model employed at this stage<sup>14</sup> stipulated a single polydisperse melt characterized by a Schulz-Zimm distribution with specified values of  $M_n$  and  $M_w$  (see above) and assumed, in the absence of entanglements in our systems, an inverse proportionality of  $D$  to  $M$ . (In view of the results to be discussed below, a reptative  $M^{-2}$  proportionality was also attempted. The fits obtained were generally somewhat inferior, and the polymer diffusion coefficients were not substantially altered.) An adjustment to the echo amplitude of each molecular fraction for the  $M$  dependence of  $T_2$  within the ensemble was always made; the measured average  $T_2$  at the curing stage of interest was supplied to the program. The only parameter being fitted was  $D(M_n)$ , the diffusion coefficient of molecules having the momentarily appropriate molecular weight  $M_n$ , all other diffusion rates scaling accordingly.

As the cure progresses, larger molecular aggregates begin to form and  $D(M_n)$  decreases as  $M_n$  increases, branching occurs, and some chain-end free volume is consumed, with an attendant increase in the glass transition temperature. In our systems the diffusion of the polymer ensemble began to be clearly distinct from that of the probe species at a conversion of about 0.3; beyond this point the model employed<sup>14</sup> added to the earlier model another component of adjustable amplitude and a single adjustable diffusion rate, raising the number of fitted parameters to three. While the amount of probe species and free curative was known, its  $T_2$  relative to that of the polymer was not independently measurable in the limited time available between diffusion measurements, so that the fit of its relative echo amplitude could not be obviated.

It is of interest to estimate the extent  $x_c$  of the curing reaction at which the amount of unreacted DDS has fallen to the level of the probe species; beyond this point the diffusion rate of the faster moving component will mainly reflect the motions of the probe molecules. Given the initial weight fraction of each (see Table I) it is only necessary to account for the decrease of free DDS by the factor  $(1 - x_c)$ .<sup>4</sup> The results are  $x_c(\text{DGEBA}) = 0.39$  and  $x_c(\text{DGEBA}) = 0.21$ , fortuitously both in the vicinity of  $x = 0.3$ , below which polymer diffusion was indistinguishable from that of the smallest molecules. An additional simplification in our data reduction results from the similarity of molecular weights and shapes of DDS and the probes (plasticizer or unreactive monomer), so that the two free diffusion rates could be subsumed in the single rate characteristic of the main probe species present, a fact which assumes greater importance above  $x_c$ . Several independent checks confirmed that our data reduction propagates no artifacts of the gradual disappearance of free DDS.

When a true network begins to form at the gelation point, it is desirable to choose a spin-echo time  $\tau$  sufficiently long to exclude contributions from the (nondiffusing and less segmentally mobile) gel fraction, to avoid difficult corrections to the sol diffusion rate.<sup>10</sup> Our choice of  $\tau = 25$  ms for all measurements represented the best compromise between this consideration and the requirement for sufficient signal strength. Beyond the gelation point the polymer diffusion rate extracted via the unaltered model thus described the desired sol diffusion. However, at later stages in the cure the molecular aggregates become so large, highly branched, and immobile that their  $T_2$  relaxation times begin to approach that of the network. The extraction of sol diffusion rates under such conditions can no longer avoid the highly uncertain corrections for the network echo contribution. Rather than altering instrument settings or pulse programs we chose to ignore polymer diffusion beyond this point but to continue with probe diffusion by invoking a simpler model, which combined all polymer echo into a single essentially unattenuatable fraction as correction to the attenuatable probe echo.<sup>26</sup> The adjustable parameters here were  $D(\text{probe})$  and the unattenuatable echo fraction. When in the final stages of the experiment all polymer echo at 50 ms had vanished, it became possible to postulate a single adjustable diffusing species,<sup>26</sup> i.e., the probe molecules.

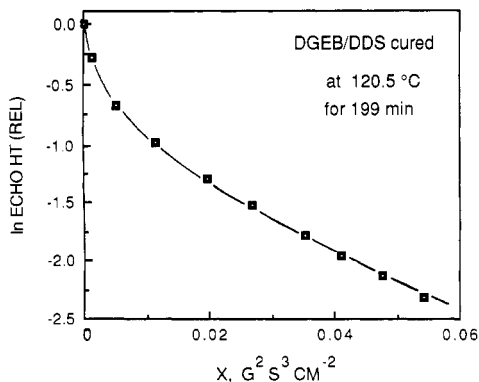


**Figure 1.** Diffusional echo attenuation (symbols) in Epon 828, 2.5 h after beginning of cure with DDS at 120 °C. Ordinate represents logarithm of spin-echo amplitude; abscissa denotes the gradient parameter  $(\delta G)^2 (\Delta - \delta/3)$  with corrections for a small steady gradient applied at all times. Model fitted (line) postulates a single fast-diffusing diluent (visible as steeper slope near origin) within a polydisperse unentangled diffusing polymer (see text).

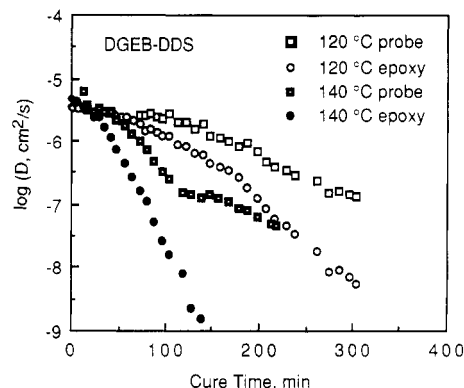


**Figure 2.** Diffusion coefficient of unreactive impurities (squares) and DGEBA aggregates of number-average molecular weight (circles) during cure with DDS, at 120.2 (open symbols) and 140.2 °C (bold symbols), as function of time from beginning of cure. At early times plasticizer and polymer diffusion are not distinct, although polydispersity is already evident.

A separate measurement of the diffusion of concentrated sol after extraction was not performed. Such an approach would yield much more rapid rates, resembling those obtained in the early stages of curing, because it does not reflect the complex interaction between sol and the gel host, information which this study was designed to elicit.

### III. Results and Discussion

**A. Time Dependence of Diffusion and Curing Reaction.** A typical echo attenuation plot is shown in Figure 1. This example for the Epon-DDS system shows the most complex interpretive model fit, permitting the extraction of two diffusion coefficients and the relative echo intensity of the fast-diffusing component; the last cannot be effectively utilized in the further analysis but serves as a check since it constitutes an upper limit on the relative amount of probe molecules present.

Figure 2 shows the time dependence of polymer as well as probe diffusion coefficients during curing in the DGEBA-DDS system at both temperatures. As is found in some curing systems<sup>3</sup> (but in sharp contrast with others differing greatly in gelation and vitrification behavior<sup>14</sup>), the decrease of molecular motions accelerates as the cure progresses, although this acceleration is less for the probe molecules than for the polymer. Identical observations apply to the results for the Epon 828-DDS system, shown in Figure 3. For both systems curing progresses more

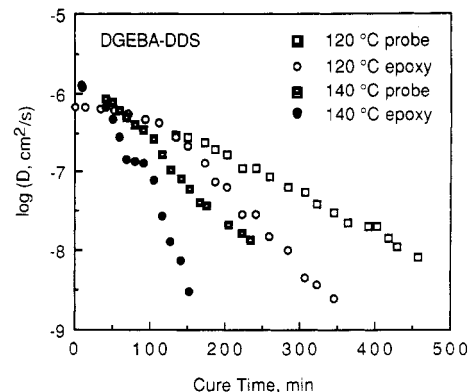


**Figure 3.** Cure time dependence of diffusion coefficient of plasticizer (squares) and Epon 828 aggregates of number-average molecular weight (circles) during cure with DDS, at two temperatures. Symbols and conventions are as in Figure 2.

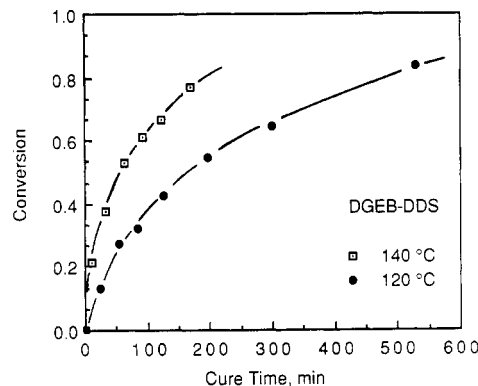


**Figure 4.** Extent of cure of DGEBA-DDS system as determined from infrared absorption data, as function of cure time at 120 (circles) and 140 °C (squares).

rapidly, and diffusion of both components is faster, at the higher temperature.

Figure 4 shows sample results of the parallel IR investigation to determine the extent of the curing reaction as function of cure time; data for the DGEBA-DDS system at both cure temperatures are displayed. (These measurements combined with branching theory provided the basis for the polydispersity modeling required for the extraction of  $D(\bar{M}_n)$  from the echo attenuation data shown in Figures 2 and 3.) For both the Epon as well as the DGEBA system equal conversions are reached  $2.5 \pm 0.3$  times faster at the higher of the two temperatures. Since this factor is only slightly greater than that ( $1.8 \pm 0.2$ ) by which corresponding diffusion coefficients differ between these temperatures, the progress of curing after its initial stage seems to be controlled more by diffusion than by the chemical reaction rate, whose temperature dependence might be expected to be less pronounced.

**B. Dependence of Diffusion on Extent of Cure.** The hypothesis of a diffusion-dominated curing rate at intermediate stages of curing is supported by a direct juxtaposition in the form of master plots in which conversion  $x$  (interpolated from the IR measurements at cure times corresponding to diffusion measurements) is used as abscissa, with the reduced diffusion rate  $D(x)/D(x=0)$  as ordinate. As may be seen from Figures 5 and 6, results for the two temperatures are superimposed for both systems; nontrivial adherence to master curves extends from  $x = 0.3$  to well beyond the putative gelation point. More detailed justification of this view will be given near the end of section III.B (below).

As discussed earlier, the gel point for both systems is calculated to occur near  $x = 0.57$ – $0.60$ . While polymer

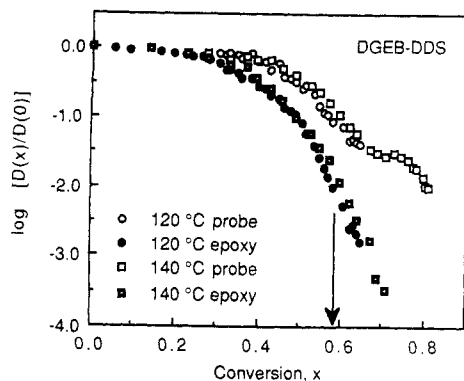


**Figure 5.** Dependence of the reduced diffusion coefficient  $D(x)/D(x=0)$  for the DGEB-DDS system on the extent  $x$  of the curing reaction as determined via IR. Results for probes (open symbols) and polymers (bold symbols) at both temperatures replotted from Figure 2 follow master curves. Mark indicates lower limit for theoretically estimated gel point.

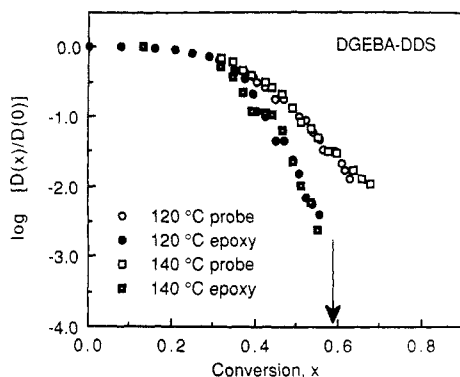


**Figure 6.** Master curve of reduced diffusion coefficients vs extent of cure for the Epon 828-DDS system. Data of Figure 3 are replotted as in Figure 5.

(i.e. sol) diffusion beyond this point rapidly becomes unobservable especially in the Epon system, probe diffusion remains measurable for some time. However, neither sol nor probe diffusion nor their general trends change abruptly as a result of gelation. This observation is in contrast with bulk mechanical measurements but is quite characteristic of diffusion and other microscopic measures, which are indifferent to the existence of large-scale molecular structures until these constitute effective topological constraints for the smaller diffusing entities.

The extraction of the range of polymer diffusion rates beyond the gel point must rely on estimates of the  $M$  distribution of the sol. While beyond gelation the sol's  $M$  averages are known<sup>28</sup> to decrease continuously as the curing reaction progresses, the ratio  $\bar{M}_w/\bar{M}_n$ , of principal concern in our data reduction,<sup>14</sup> appears to be relatively constant, in the range of 2–3; on this basis we continued to obtain excellent fits to the echo attenuation data. Because of the smaller molecular weights involved, diffusion in the DGEB system was observable to higher conversions than in the Epon system, particularly at 140 °C. We believe that the small irregularities in  $D(\text{probe})$  in this case near  $x = 0.7$  are not associated with gelation but rather represent an artifact of the switch between the use of different data reduction models (see above) as sol diffusion became unobservable.

Adherence of the data to the master plots is not limited to the polymers but extends to the probe molecules as well. This fact suggests that the diffusion rates in both of our systems contain a major contribution common to polymer and probe, the most obvious candidate

being the free volume accessible to diffusive jumps. The free volume is understood<sup>29</sup> to be locally redistributable at no cost in energy and is thus (at least in the simplest versions of the theory) equally available to all diffusing species.

This interpretation is helpful in estimating one of the contributions to the decrease of polymer diffusion rate as the cure progresses. Probe molecules, being unreactive and present in relatively small and unchanging concentration, accurately measure intermolecular friction at any time during curing. Unless the probe molecules are large or complex enough to experience substantial restraint by emerging host entanglements or cross-linking (not expected to be the case in the present study), the only significant change in friction they experience is due to the changing free volume. If, moreover, the polymer and probe molecules are monomerically equivalent or similar (as is the case here; adherence to the master curves supports this contention), we expect that free-volume changes will retard polymer and probe diffusion rates by approximately the same numerical factor.<sup>30</sup> A comparison of probe and polymer diffusion in Figures 5 and 6 thus suggests that up to half of the decrease in  $\log D(\text{polymer})$  during cure arises from the depletion of free volume, with the remainder to be accounted for in terms of the increase of polymer molecular weight, polymer branching, and interference between diffusing polymer molecules and the emerging (entangled or cross-linked) gel. In the next section an attempt will be made to estimate the relative contributions of these effects.

It is not difficult to assign the cause of the substantial decrease in free volume as the cure progresses. A major contribution to polymer free volume is associated with unattached ends of molecules, e.g. polymer chain ends. This contribution has been shown to account for the difference in free volume, as well as diffusion rate as its sensitive indicator, between otherwise identical melts of differing molecular weight.<sup>31</sup> Free chain ends, relatively abundant at the beginning of cure, are rapidly consumed as a result of the formation of molecular aggregates (chain extending and branching), virtually disappearing at the completion of the cure.

Given the strong dependence of  $D$  on fractional free volume,<sup>29,32</sup> the observed decrease of probe diffusion rate amounting for both systems to some 2 orders of magnitude may be crudely estimated to correspond to a decrease in free volume by perhaps one-third, which may therefore be regarded as a reasonable upper limit on relative chain-end free volume prior to curing. However, while for both systems probe and polymer diffusion rates become distinguishable near  $x = 0.3$ , at some later fixed  $x$  (e.g., the gel point)  $\log D(\text{probe})$  in Epon 828 has decreased by twice the amount observed in the DGEB system. This observation is in accord with the free-volume interpretation given the differences in initial chain-end density and demonstrates that probe diffusion remains observable until the free volume has decreased to some critical value apparently common to both systems. It further implies that the correction of polymer diffusivity for free-volume changes will be much more severe in the Epon system.

The dependence of diffusion on free volume, as evidenced here directly in the case of probe diffusion, is known<sup>29</sup> to have the approximate form  $D \sim e^{-1/F}$ . The fractional free volume  $F$  increases with rising temperature above  $T_g$  in a pronounced, linear manner. It is easily shown that  $D(T)$  with appropriate free-volume parameters can have an equally or more pronounced tempera-

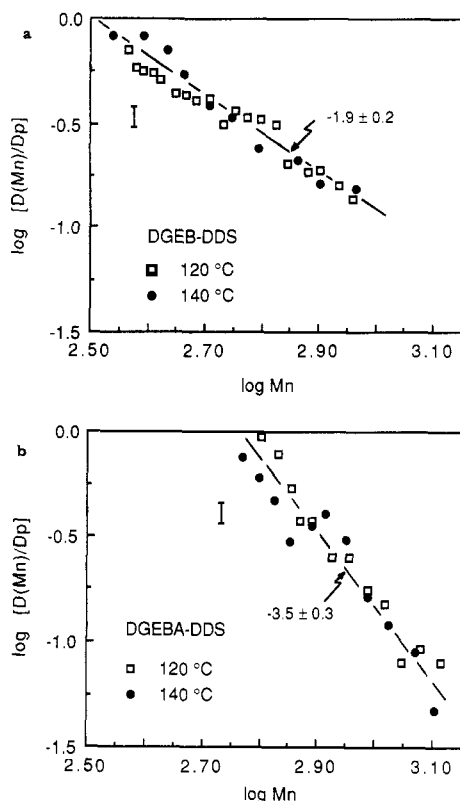


**Figure 7.** Polymer diffusion coefficients corrected for free-volume changes  $[D_{\text{cfv}}(\bar{M}_n)]$ ; see eq 2] for the DGEBA-DDS system (a) and the Epon 828-DDS system (b), as function of the theoretical number-average molecular weight of the polymer aggregates during curing prior to gelation. Data at 120 and 140 °C are included; bar denotes uncertainty. Power-law slopes are indicated.

ture dependence than that of a chemical reaction rate following the Arrhenius law with a typical thermal activation energy. Our conclusion that the curing reaction in our systems for  $x > 0.3$  is largely limited by diffusion rather than by chemical reactivity is based on the observation (Figures 2, 3, 5, and 6) that the increasing polymer diffusion rate at the higher temperature is approximately matched by the reduction of the times scale for attaining equal values of  $x$ , in both systems over the entire accessible range of  $x > 0.3$ . While this observation is an elementary consequence of Fickian diffusion, reproducing this observed behavior via the temperature dependence of the chemical reaction rate would require ad-hoc assumptions.

**C. Dependence of Diffusion on Molecular Weight Prior to Gelation.** For a separation of polymer diffusion into its contributions, it will be advantageous to represent the results in a form suitable for direct comparison with molecular weight power laws. The probe molecules, whether present in trace concentrations or, as here, in finite amounts, should not be expected to obey diffusional power-law behavior in polymer molecular weight, but their diffusion rates may be used to correct polymer diffusion for the changing free volume. The quantity plotted in Figure 7 is therefore

$$D_{\text{cfv}}(\bar{M}_n, x) = \frac{D(\bar{M}_n, x)D(\text{probe}, 0)}{D(\bar{M}_n, 0)D(\text{probe}, x)} = \frac{D(\bar{M}_n, x)}{D(\text{probe}, x)} \quad (2)$$

The second equality, while not valid in principle, is a consequence here of the indistinguishability of probe and polymer diffusion rates in the earliest stages of the cure.  $D_{\text{cfv}}(\bar{M}_n)$  is independent of temperature and is displayed

as function of the theoretical number-average molecular weight of the polymer,  $\bar{M}_n(x)$ , up to gelation. The advantages of plotting  $D(\bar{M}_n)$  vs  $\bar{M}_n$  over the use of some other molecular weight average for abscissa and ordinate have been discussed in detail elsewhere;<sup>14</sup> of particular importance here is the relative lack of dependence of  $D(\bar{M}_n)$  on the dispersity ratio  $\bar{M}_w/\bar{M}_n$  because that quantity undergoes substantial increase during curing, a circumstance that would otherwise invalidate quantitative interpretation of power-law plots.<sup>33</sup>

Examination of Figure 7 shows that for both systems  $D_{\text{cfv}}$  decreases with increasing  $\bar{M}_n$  in a manner consistent within experimental error with simple power-law behavior, if this term is still appropriate in view of the limited molecular weight range. It begins at the point at which polymer and probe diffusion first become distinct, i.e., at about 1.5 times the initial polymer molecular weight ( $M \approx 300$  for DGEBA-DDS and 600 for Epon-DDS). The  $M$  exponent varies between systems, taking the values  $-1.9 \pm 0.2$  for DGEBA-DDS and  $-3.5 \pm 0.3$  for DGEBA-DDS. Thus the decrease of  $D_{\text{cfv}}$  in the Epon system begins at roughly twice the molecular weight and is approximately twice as steep as for DGEBA, at least up to the gel point, in spite of the much larger free-volume correction in Epon 828. Since the concentrations and molecular weights of the probe molecules are relatively similar, these differences are likely to be attributable to the host system.

The Rouse model<sup>34</sup> of the dynamics of unentangled polymer systems makes predictions for various dynamical quantities, most of which depend on the architecture of the molecules. Significantly, its prediction for the simplest case, center-of-mass self-diffusion of polymer molecules in solvents consisting of small molecules, is independent of architecture, applying equally to linear and branched polymers. On the basis of that model, the molecular weight dependence of  $D(\text{polymer})$  in the form of a power-law slope would be no steeper than  $-1$ . This slope might be further flattened as a hydrodynamic result of branching, as the radius of gyration rises less rapidly with molecular weight than for linear molecules.<sup>35</sup>

Reptation theory<sup>36</sup> demands a slope of  $-2$ , but its central prerequisite is the existence of entanglements of the diffusing species with the host species (here identical). Formation of a coherent network has not occurred prior to gelation, so that entanglement effects on  $D(\bar{M}_n)$  should become observable only when  $\bar{M}_n$  begins to exceed a critical molecular weight  $M_c$  somewhat in excess of the entanglement spacing  $M_e$  for these polymer species.<sup>29</sup> While  $M_c$  is not well-known for epoxies, comparison with similar polymers suggests that for our systems it should be far enough above  $\bar{M}_n$  up to gelation so that the possibility of reptative behavior would seem to be remote. A model polydispersity calculation<sup>14</sup> assuming linear molecules suggests that any melt with  $\bar{M}_n < 1400$  and  $M_c > 5000$  (appropriate for the Epon 828 system) should remain entirely unentangled until  $\bar{M}_w$  rises above 15 000 (exact results depending on the detailed form of the  $M$  distribution). In fact, the assumption of linear molecules is more conducive to entanglement than is the branching which must occur in our systems. Thus, entangled behavior in the Epon system should not appear until very near the gel point, whereas the observed slope is already well established at the much lower conversion of 0.4. Significant incidence of cyclization (with or without physical interlinking of the cyclic aggregates) also would only be expected immediately preceding gelation.

The growing dispersity of the molecular aggregates is not a source of artifacts in the diffusional  $M$  depen-



dence. As described above, polydispersity is accounted for in two ways: the primary data reduction applies models of the polydispersity based on the theoretical  $M$  distribution appropriate at the given stage of curing, and all further data interpretation is based on a molecular weight reference average chosen to leave  $D(M_{\text{ref}})$  independent of polydispersity at fixed  $M_{\text{ref}}$ . On the basis of earlier numerical simulations<sup>14</sup> we use the approximately optimal  $M_{\text{ref}} = \bar{M}_n(x)$ , ensuring that the slopes in Figure 7 are not affected by the increase in dispersity.

We are thus confronted by evidence that the effective friction coefficient, after correction for free-volume changes and in the probable absence of reptation, increases as the cure progresses and that this increase is more pronounced in the system having greater molecular weight between branch points. Since in a melt host and diffusant species are the same, no significant changes in collision dynamics or effective solvent quality can attend the growth of molecular aggregates and no changes in the experiment's effective reference frame (e.g. between polymer-fixed and laboratory-fixed) can occur. The remaining possibility is a pronounced change in the mechanism of center-of-mass diffusion as branching occurs. It may be expected that branching will retard the progress of any given molecular aggregate in two ways, by lessening its ability to evade constraints by neighboring molecules and by inhibiting those molecules in their accommodation of the passage of a diffusing fragment. An unambiguous separation of the effects of branching into diffusant and host effects will, however, not be possible.

It has often been postulated that the transition from Rouse to reptation behavior cannot be very sharp because of the limited number of degrees of freedom involved in a diffusive segmental jump. While reptation cannot fully develop until the minimum conditions for entanglement have been greatly exceeded, some rudimentary tubelike lateral constraints to segmental motion might anticipate full entanglement. It is conceivable that in melts of branched molecules the width of the entanglement transition may be much greater than for linear molecules, with the special caution that molecules containing long branches are known<sup>37</sup> to be prevented from reptating and must depend for their diffusive motion on arm retraction and/or the renewal and reorganization of the host tubes constraining the arms. Such a hypothesis would lead for short-branched melts to  $M$  exponents approaching reptation model behavior (e.g. Figure 7a) and for long-branched melts to  $M$  exponents in excess of  $-2$  (e.g. Figure 7b) on their way to an exponential  $M$  dependence rather than power-law behavior. Our limited diffusion data beyond gelation are more difficult to interpret but seem to be consistent with this general picture.

Apparent support for an interpretation along these lines is supplied by a recent study of the diffusion of star-branched polymers in concentrated solutions,<sup>38</sup> which has obvious analogies to the present case. Its authors conclude that as such solutions become entangled, a relatively gradual transition from a hydrodynamic to a topology-constrained diffusion mechanism occurs, in which star-branched polymers are retarded significantly by comparison with linear polymers of equal molecular weight as their degree of entanglement with the matrix increases. The pronounced dependence of diffusion rate on architecture in entangled polymer systems at present relies on the reptation/tube picture for a satisfactory explanation. But even for linear polymers apparently innocuous changes in host topology appear to play a significant role: a recent investigation<sup>39</sup> has shown that the replace-

ment of periodically positioned cross-links by randomly spaced ones can change the  $M$  exponent of diffusion for linear polymers entangled with the network from  $-2$  to  $-3$ .

However, rather than postulating an unlikely substantial displacement of the entanglement transition to the low oligomeric range, we concur with the more orthodox interpretation that both of our systems remain entirely unentangled prior to gelation. Thus we view the sharp decrease of polymer diffusion rate during curing as an instance of inapplicability of the Rouse theory. While that theory is, in fact, independent of molecular architecture in its prediction of translational friction, it presupposes diffusant molecular flexibility and the presence of a simple viscous host medium. The presence of relatively inflexible branches in both diffusant and host is likely to result in violation of both conditions, more serious in the DGEBA system because of its longer branching unit.

We are not aware of analytical alternatives applicable in such cases; for the present the analysis of diffusion in melts of unentangled but rigid branched molecules appears relegated to collision-dynamic calculational approaches. It seems safe to deduce, however, that the difference between the observed power-law exponents and that predicted by the Rouse model, perhaps with a minor adjustment for the reduction of the radius of gyration at a given  $M$  as a result of branching, is directly attributable to the topological effects of branching. It must contain contributions from two interrelated causes, the extra difficulty of passage of a diffusing molecule due to its own branching and the decreased cooperation among nearby equivalent host molecules due to their branching, but the relative effectiveness of each is still a matter of conjecture.

#### IV. Summary and Conclusions

We have measured the self-diffusion of polymer and probe molecules, including free curing agent, of two epoxies differing in molecular weight during curing to well beyond the gel point. Parallel IR reaction studies permitted correlation of the diffusion results with extent of the curing reaction and, via branching theory, with the molecular weight distribution up to gelation. The interpretation of these experiments attempted to separate the various influences on the monomeric friction constants of the polymer. The effects considered were the decrease of chain-end free volume as a result of curing, Rouse-like behavior in analogy with linear polymers, the possibility of reptation and its prevention in long-branched molecular aggregates, and other possible changes in segmental diffusive mobility as a result of branching. The results and principal interpretations of this study may be summarized as follows:

(1) The spin-echo attenuation plots are satisfactorily reproduced by using models stipulating, in the most general case, a monodisperse fast-diffusing species (probe: impurity, plasticizer, free curing agent) and a slower diffusing polydisperse species (polymer melt, aggregates, sol). Probe and polymer diffusion in both systems become distinct near a cure extent  $x = 0.3$ . At any stage of curing the observed polymer diffusivity distribution is in semi-quantitative accord with the known or theoretical molecular weight distribution.

(2) The progress of the cure at  $x > 0.3$  is largely controlled by diffusion. The rate of attaining equivalent extents of cure at  $140^\circ\text{C}$  is more than twice as great as at  $120^\circ\text{C}$ , whereas polymer as well as probe diffusion rates increase by a factor of slightly less than 2. For both

systems plots of normalized diffusivities vs  $x$  produce master curves superimposing results for the two temperatures.

(3) The gel point is not discernible on the basis of the diffusion data. For both systems probe diffusion and its rate of decrease are continuous across the gel point; the same is true for DGEBA diffusion, where a sol echo is measurable.

(4) The consumption of chain-end free volume as a result of curing reduces the diffusion rate of probe molecules by some 2 orders of magnitude before probe diffusion measurements become imprecise well beyond the gel point. At a given  $x$  the decrease in probe diffusivity is much more pronounced in the Epon system, in keeping with differences in initial  $M$  and hence initial chain-end free volume and ultimate cross-link density. Polymer diffusion may be assumed to be affected by free volume to the same extent as probe diffusion. Free-volume considerations also contribute to the factor of 5 by which diffusion of DGEBA exceeds that of Epon 828 prior to curing.

(5) The free-volume-corrected polymer diffusion rate  $D(M_n)$  follows a power law in molecular weight  $\bar{M}_n(x)$ , over the range  $0.3 > x > 0.6$  (estimated gel point). The  $M$  exponent for both systems far exceeds the predictions of the Rouse model. While this behavior is not quantitatively understood, it must reflect a change in diffusion mechanism related to branching, i.e., the formation of rigid branched molecular aggregates during curing. This effect confirms the inapplicability of the Rouse model to these systems and is more pronounced in the DGEBA system due to its longer branches.

(6) The combination of polymer self-diffusion, probe self-diffusion, and an independent measure of the progress of the curing reaction, e.g. IR, represents a powerful set of tools for the study of curing of polymers above the glass transition. We believe the present curing study to be the first to use this combination; the pulsed-gradient spin-echo technique was indispensable in this task.

Related studies of molecular mobility in epoxy-based composites during and after cure are in progress and involve NMR  $T_2$  relaxation as an additional technique.

**Acknowledgment.** We wish to thank W. Mattice and F. N. Kelley for their encouragement of this work and for several valuable discussions about the nature of the curing process in epoxies and the latter for supplying some sample materials. We are indebted to T. Lodge for his critical reading of the manuscript and his cogent analysis of the theoretical basis of polymer diffusion models. G. Iannacchione was helpful with aspects of sample preparation and data analysis. We express our gratitude to Thiokol Corp. for continuing support of this line of investigation under their University I. R. & D. program, and particularly to J. Bennett for his guidance and encouragement. Support of this project by the National Science Foundation is gratefully acknowledged.

## References and Notes

- (1) Gillham, J. K. In *Encycl. Polym. Sci. Eng.* 1986, 4, 519.

- (2) Venkataraman, S. K.; Coyne, L.; Chambon, M.; Gottlieb, M.; Winter, H. H. *Polym. Prepr. (Am. Chem. Soc., Div. Polym. Chem.)* 1988, 29, 571.
- (3) Fanconi, B. M.; Wang, F. W.; Hunston, D. L. *Proc. ANTEC* 87, 1987, 1100.
- (4) Scarlata, S. F.; Ors, J. A. *Polym. Commun.* 1986, 27, 41.
- (5) George, G. A.; Schweinsberg, D. P. *J. Appl. Polym. Sci.* 1987, 33, 2282.
- (6) Stroeks, A.; Shmorhun, M.; Jamieson, A. M.; Simha, R. *Polymer* 1988, 27, 467.
- (7) Senturia, S. D.; Sheppard, N. F., Jr. *Adv. Polym. Sci.* 1986, 80, 1.
- (8) Yu, W. C.; Sung, C. S. P. *Macromolecules* 1988, 21, 365.
- (9) Dušek, K.; Spěváček, J. *Polymer* 1980, 21, 750.
- (10) von Meerwall, E.; Stone, T. J. *Polym. Sci., Polym. Phys. Ed.* 1989, 27, 503.
- (11) Larson, D. W.; Strange, J. H. *J. Polym. Sci., Polym. Phys. Ed.* 1973, 11, 65.
- (12) Larson, D. W.; Strange, J. H. *J. Polym. Sci., Polym. Phys. Ed.* 1973, 11, 449.
- (13) Larson, D. W.; Strange, J. H. *J. Polym. Sci., Polym. Phys. Ed.* 1973, 11, 1453.
- (14) von Meerwall, E. D.; Palunas, P. J. *Polym. Sci., Polym. Phys. Ed.* 1987, 25, 1439.
- (15) von Meerwall, E. D.; Shook, D.; Min, K. J.; Kelley, F. N. *J. Appl. Phys.* 1984, 56, 2444.
- (16) Yu, W. C.; von Meerwall, E. *Bull. Am. Phys. Soc.* 1989, 34, 855.
- (17) Yu, W. C.; von Meerwall, E.; Mattice, W.; Kelley, F. N. *Bull. Am. Phys. Soc.* 1989, 35, 54.
- (18) Dušek, K.; Ilavský, M. *J. Polym. Sci. Symp.* 1975, 53, 29.
- (19) Miller, D. R.; Macosko, C. W. *Macromolecules* 1980, 13, 1063.
- (20) Bidstrup, S. A.; Macosko, C. W. In *Proc. & Discuss., 1986 Conference on Crosslinked Epoxies*; Sedláček and Kahovek, Eds.; Berlin, FRG, 1987; p 253.
- (21) Matejka, L.; Dušek, K. In *Proc. & Discuss., 1986 Conference on Crosslinked Epoxies*; Sedláček and Kahovek, Eds.; Berlin, FRG, 1987; p 107.
- (22) Stejskal, E. O.; Tanner, E. J. *J. Chem. Phys.* 1965, 42, 288.
- (23) von Meerwall, E. *Rubber Chem. Technol.* 1985, 58, 527.
- (24) von Meerwall, E. D.; Burgan, R. D.; Ferguson, R. D. *J. Magn. Reson.* 1979, 34, 339.
- (25) von Meerwall, E. D.; Ferguson, R. D. *J. Appl. Polym. Sci.* 1979, 23, 877.
- (26) von Meerwall, E.; Ferguson, R. D. *Comput. Phys. Commun.* 1981, 21, 421.
- (27) von Meerwall, E. D.; Kamat, M. *J. Magn. Reson.* 1989, 83, 309.
- (28) Miller, D. R.; Valles, E. M.; Macosko, C. W. *Polym. Eng. Sci.* 1979, 19, 272.
- (29) See, for example, Ferry, J. D. *Viscoelastic Properties of Polymers*, 3rd ed.; Wiley: New York, 1980.
- (30) von Meerwall, E. D.; Amis, E. J.; Ferry, J. D. *Macromolecules* 1985, 18, 260.
- (31) von Meerwall, E. D.; Grigsby, J.; Tomich, D.; Van Antwerp, R. *J. Polym. Sci., Polym. Phys. Ed.* 1982, 20, 1037.
- (32) Cohen, M. H.; Turnbull, D. *J. Chem. Phys.* 1959, 31, 1164.
- (33) Bernard, D. A.; Noolandi, J. *Macromolecules* 1983, 16, 548.
- (34) For a review of this subject, see: Klein, J. *Contemp. Phys.* 1979, 20, 611.
- (35) See, for example: von Meerwall, E.; Tomich, D. H.; Grigsby, J.; Pennisi, R.; Fetters, L. J.; Hadjichristidis, N. *Macromolecules* 1983, 16, 1715.
- (36) The conditions for reptation and its principal results are reviewed in: Tirrell, M. *Rubber Chem. Technol.* 1984, 57, 523.
- (37) Graessley, W. W. *Adv. Polym. Sci.* 1982, 47, 67.
- (38) Lodge, T. P.; Markland, P.; Wheeler, L. M. *Macromolecules* 1989, 22, 3409.
- (39) Baumgartner, A.; Muthukumar, M. *J. Chem. Phys.* 1987, 87, 3082.

**Registry No.** Epon 828, 25068-38-6; DBP, 84-74-2; DGEBA, 2425-79-8; DDS, 80-08-0.